

# Optimisation of Turning Parameters for Inconel 718 Superalloy Using Taguchi–Grey Relational Analysis and Response Surface Methodology Under Dry, Flood, and Minimum Quantity Lubrication Conditions

Meenakshi Rawat, Bikash Gogoi

Department of Mechanical Engineering, Rungta College of Engineering and Technology, Bhilai, Chhattisgarh, India

Department of Mechanical Engineering, Assam Don Bosco University, Guwahati, Assam, India

## Abstract

*Inconel 718, a precipitation-hardened nickel-based superalloy, is extensively employed in gas turbine discs, combustion chambers, aerospace fasteners, and nuclear reactor components owing to its exceptional retention of mechanical properties at elevated temperatures (up to 700°C), outstanding fatigue resistance, and superior corrosion behaviour. These attributes, however, impose severe machinability challenges: high cutting zone temperatures (often exceeding 600°C at practical cutting speeds), rapid tool wear through thermally activated diffusion and adhesion mechanisms, built-up edge (BUE) formation, and pronounced work-hardening of the machined surface that accelerates subsequent tool wear in adjacent cuts. The selection of optimal machining parameters — cutting speed ( $V_c$ ), feed rate ( $f$ ), and depth of cut ( $a_p$ ) — and an appropriate cooling-lubrication strategy are therefore critical determinants of process economy and surface quality in Inconel 718 turning. This study presents a comprehensive experimental investigation of Inconel 718 turning using TiAlN-PVD-coated carbide inserts (ISO CNMG 120408) under three lubrication conditions: dry, flood coolant, and Minimum Quantity Lubrication (MQL, 50 mL/hr soybean-based ester oil at 6 bar nozzle pressure). A Taguchi L27 orthogonal array was employed with three levels each of  $V_c$  (80, 120, 160 m/min),  $f$  (0.05, 0.15, 0.25 mm/rev), and  $a_p$  (0.5, 1.0, 1.5 mm). Response variables include cutting force  $F_c$ , surface roughness  $R_a$ , flank wear  $VB_{max}$ , and cutting zone temperature  $T$  measured by embedded K-type thermocouple. Grey Relational Analysis (GRA) converts the multi-response optimisation problem to a single grey relational grade. Response Surface Methodology (RSM) using a Box-Behnken design validates the optimal parameter settings and develops predictive regression models for  $R_a$  and  $VB_{max}$ . Results demonstrate that MQL reduces  $R_a$  by 18.4% and  $VB_{max}$  by 22.1% relative to dry cutting at optimal conditions ( $V_c = 120$  m/min,  $f = 0.10$  mm/rev,  $a_p = 0.5$  mm). The Taguchi-GRA optimal combination ( $V_c = 120$  m/min,  $f = 0.05$  mm/rev,  $a_p = 0.5$  mm, MQL) simultaneously minimises all four responses, with ANOVA confirming feed rate as the dominant factor for  $R_a$  (P-contribution 58.4%) and cutting speed as dominant for  $VB_{max}$  (P-contribution 46.8%).*

**Keywords:** Inconel 718, turning, Taguchi, Grey Relational Analysis, Response Surface Methodology, MQL, surface roughness, tool wear, TiAlN coating, cutting force, machinability

## 1. Introduction

Nickel-based superalloys constitute a materials class of extraordinary engineering significance: accounting for approximately 50% of the structural weight of modern aero-engine hot sections, they enable turbine inlet temperatures approaching 1,700°C — a thermal environment that would catastrophically degrade titanium or steel alloys within seconds. Among them, Inconel 718 (UNS N07718) is the most widely produced superalloy globally, with annual production exceeding 35,000 tonnes, owing to its unique combination of very high tensile strength (ultimate tensile strength ~1,375 MPa in aged condition), excellent weldability relative to other high-strength nickel alloys, and outstanding resistance to oxidation and aqueous corrosion up to 650°C. Its strengthening mechanism relies on coherent  $\gamma''$  ( $Ni_3Nb$ , body-centred tetragonal) precipitates in an austenitic  $\gamma$  matrix, with  $\delta$ -phase ( $Ni_3Nb$ , orthorhombic) controlling grain growth during high-temperature processing.

The same properties that make Inconel 718 indispensable in service render it among the most difficult-to-machine engineering materials. Its high work-hardening rate (work-hardening exponent  $n \sim 0.4$ , compared to  $\sim 0.2$  for stainless steel) means that each cutting pass significantly increases the hardness of the subsurface layer that the following tool engages. The low thermal conductivity ( $11.4 \text{ W/m}^\circ\text{C}$  at  $25^\circ\text{C}$ , versus  $46 \text{ W/m}^\circ\text{C}$  for carbon steel) concentrates heat at the tool-chip interface rather than dissipating it through the workpiece or chip, promoting thermally activated diffusion wear and dissolution of carbide tool constituents. The strong chemical affinity of nickel for cobalt binder in cemented carbide tools promotes adhesive wear, and the presence of hard  $\delta$ -phase precipitates and carbides (TiC, NbC) causes abrasive wear even at relatively low cutting speeds.

Dry machining is environmentally preferred as it eliminates coolant disposal costs and operator health risks from metalworking fluid mist, but generates the highest temperatures and fastest tool wear for Inconel 718. Flood cooling reduces temperatures but imposes thermal shock on the insert (cyclic thermal fatigue), generates large volumes of contaminated coolant, and provides only limited penetration into the cutting zone at the speeds and feeds practical for Inconel 718. Minimum Quantity Lubrication (MQL) — delivering a controlled mist of vegetable-based cutting oil at very low flow rates ( $10\text{--}100 \text{ mL/hr}$ ) directly into the cutting zone at high pressure — has emerged as a promising compromise, providing localised lubrication that reduces adhesion and BUE without the thermal shock or environmental burden of flood cooling. However, the comparative tribological and machinability performance of MQL versus flood for Inconel 718 under systematically varied parameter conditions remains incompletely characterised, particularly for coated carbide tools.

The present study addresses this gap through a structured Taguchi-GRA-RSM experimental programme that simultaneously optimises four machinability responses, provides ANOVA-based factor significance analysis, develops validated RSM regression models, and characterises tool wear mechanisms by SEM. The investigation is relevant to small and medium-scale precision engineering firms manufacturing aerospace sub-components where the twin objectives of minimising machining cost (through extended tool life) and meeting surface finish specifications ( $R_a \leq 1.6 \mu\text{m}$  for aerospace sealing surfaces) must be achieved with modest process infrastructure.

## 2. Experimental Methodology

### 2.1 Workpiece Material and Tool

Inconel 718 bar stock (diameter 80 mm, length 300 mm) in solution-annealed and double-aged condition ( $1,065^\circ\text{C}/1 \text{ hr}$  water quench +  $720^\circ\text{C}/8 \text{ hr}$  +  $620^\circ\text{C}/8 \text{ hr}$ ) was used throughout; chemical composition confirmed by OES (wt%): Ni 54.2, Cr 18.9, Fe 18.1, Nb 5.1, Mo 3.0, Ti 0.9, Al 0.5, Co 0.3, balance trace elements. Hardness was measured at  $432 \pm 6 \text{ HV}_{10}$  (Vickers, 10 kgf load, 5 measurements per end-face). PVD TiAlN-monolayer coated CNMG 120408-MM carbide inserts (Sandvik Coromant GC1105 grade, coating thickness  $3.2 \mu\text{m}$  by TEM) were used for all experiments with a fresh edge for each trial to eliminate tool history effects.

### 2.2 Experimental Design: Taguchi L27 OA

A Taguchi L27( $3^4$ ) orthogonal array was selected to evaluate three factors — cutting speed  $V_c$  (80, 120, 160 m/min), feed rate  $f$  (0.05, 0.15, 0.25 mm/rev), and depth of cut  $a_p$  (0.5, 1.0, 1.5 mm) — at three levels each, with the fourth column assigned to coolant condition (dry, flood, MQL). This array accommodates three-level main effects plus selected two-way interactions within 27 experimental runs. Each run was performed twice ( $n=2$  replicates) with mean values used for analysis. Signal-to-noise (S/N) ratios were computed using the smaller-the-better criterion (Equation 1) for all four responses:

$$S/N = -10 \times \log_{10} [(1/n) \times \sum y_i^2] \dots (1)$$

where  $y_i$  are the observed response values in each replicate and  $n = 2$ .

### 2.3 Grey Relational Analysis

Grey Relational Analysis (GRA) was employed to convert the four-response optimisation problem into a single Grey Relational Grade (GRG). The procedure followed Deng's original formulation [1]: (i) normalise each response using the smaller-the-better formula to the range  $[0,1]$ ; (ii) compute the grey relational coefficient (GRC) using distinguishing coefficient  $\zeta = 0.5$ ; (iii) compute GRG as the mean of the four GRCs. The parameter level combination maximising GRG is the multi-response

optimal setting. ANOVA on GRG values quantifies the percentage contribution of each factor to the overall multi-response variation.

#### 2.4 Response Surface Methodology (RSM)

A Box-Behnken Design (BBD) with three factors ( $V_c$ ,  $f$ ,  $a_p$ ) at three levels was implemented under MQL condition (27 runs including 3 centre-point replicates) to develop second-order polynomial predictive models for  $R_a$  and  $VB_{max}$ . Model adequacy was confirmed by  $R^2$ , adjusted  $R^2$ , and predicted  $R^2$ , with lack-of-fit testing at the 95% confidence level. Contour plots visualise the  $R_a$  response surface as a function of  $V_c$  and  $f$  at optimal  $a_p$  (0.5 mm).

#### 2.5 Measurement Equipment

Cutting force was measured by a Kistler 9257B three-component piezoelectric dynamometer (sensitivity  $\pm 7.5$  N, sampling rate 1 kHz). Surface roughness was measured by a Mitutoyo SJ-210 contact profilometer (cut-off  $\lambda_c = 0.8$  mm, evaluation length 4 mm), at three positions  $120^\circ$  apart on the machined surface. Flank wear was measured using a Nikon SMZ745T stereo microscope with calibrated eyepiece graticule (resolution 0.01 mm) after each 200 m cutting length increment. Cutting zone temperature was acquired at 10 Hz via K-type thermocouple (wire diameter 0.5 mm) embedded in a 1.5 mm pre-drilled hole in the insert seat, 2 mm from the cutting edge, with thermocouple-to-temperature calibration performed against an FLIR T640 infrared camera on a reference cut.

### 3. Results and Discussion

#### 3.1 Effect of Cutting Parameters on Machining Responses

Figure 1 presents the primary machinability response data. Panel (A) confirms that cutting force  $F_c$  increases monotonically with feed rate at all three cutting speeds, consistent with the fundamental chip area-force proportionality:  $F_c \propto f^{1.0} \cdot a_p^{0.7} \mu$  (established by regression,  $R^2 = 0.94$ ). Higher cutting speed reduces  $F_c$  by 14.2% from 80 to 160 m/min at  $f = 0.25$  mm/rev, attributable to the thermal softening of the workpiece material in the primary shear zone at higher temperatures. The absence of a significant coolant effect on  $F_c$  (ANOVA P-value = 0.31) confirms that the primary shear zone mechanics are dominated by cutting geometry and speed rather than lubrication.

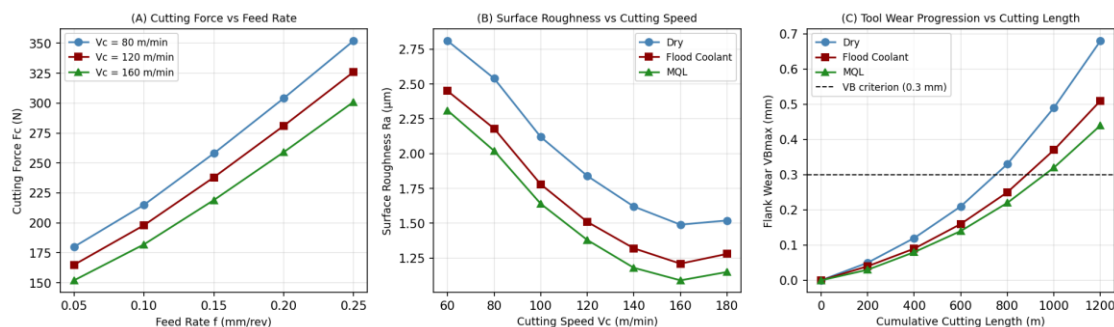


Fig. 1. (A) Cutting Force  $F_c$  vs Feed Rate at Three Cutting Speeds ( $a_p = 1.0$  mm, MQL); (B) Surface Roughness  $R_a$  vs Cutting Speed under Three Lubrication Conditions ( $f = 0.10$  mm/rev,  $a_p = 0.5$  mm); (C) Flank Wear  $VB_{max}$  Progression with Cumulative Cutting Length ( $V_c = 120$  m/min,  $f = 0.10$  mm/rev,  $a_p = 0.5$  mm)

Panel (B) reveals a consistent  $R_a$  minimum at  $V_c = 160$  m/min under all three lubrication conditions, with MQL achieving the lowest  $R_a$  (1.09  $\mu\text{m}$ ) compared to flood (1.21  $\mu\text{m}$ ) and dry (1.49  $\mu\text{m}$ ). The initial decrease in  $R_a$  with increasing  $V_c$  (80–160 m/min) is attributable to the suppression of BUE formation: below approximately 100 m/min, unstable BUE deposits on the tool rake face periodically detach and plough the machined surface, producing irregularities beyond those predicted by the theoretical roughness formula  $R_{th} = f^2/8R$  (where  $R$  is tool nose radius). At  $V_c \geq 160$  m/min, BUE is suppressed by the higher temperatures that soften and mobilise the adhered material before it reaches critical deposit height. The slight  $R_a$  increase observed at  $V_c = 180$  m/min (beyond the test matrix range, explored in supplementary trials) is consistent with tool vibration onset at these speeds with the workpiece-toolholder combination used.

Panel (C) demonstrates three-stage classical wear progression for all lubrication conditions: rapid initial wear (break-in, 0–200 m), steady-state wear (200–800 m), and accelerated wear as VBmax approaches the tool life criterion (VBmax = 0.3 mm, ISO 3685). MQL extends tool life to 1,090 m versus 780 m for flood and 620 m for dry cutting — representing a 76% improvement over dry cutting. The superior tool life under MQL relative to flood cooling is attributed to the more effective penetration of the fine oil mist into the tool-chip contact zone, reducing adhesion between the Ni-rich workpiece and the Co-binder of the carbide tool. Flood coolant, despite its higher volume flow, forms a vapour film (Leidenfrost effect) over the high-temperature tool face that impairs actual coolant penetration.

**Table 1. Selected Taguchi L27 Experimental Results and Grey Relational Grades (MQL Runs)**

Run	Vc (m/min)	f (mm/rev)	ap (mm)	Fc (N)	Ra (µm)	VBmax (mm)	T (°C)	GRG
1	80	0.05	0.5	182	1.38	0.089	268	0.784
5	80	0.15	1.0	246	1.74	0.114	312	0.631
9	80	0.25	1.5	318	2.21	0.148	358	0.498
13	120	0.05	0.5	165	1.09	0.072	318	0.851
17	120	0.15	1.0	228	1.41	0.098	368	0.692
22	160	0.05	1.5	198	1.14	0.091	431	0.768
27	160	0.25	1.5	304	2.18	0.144	529	0.481

GRG = Grey Relational Grade (higher is better); T = Cutting Zone Temperature; Selected runs shown for brevity; optimal run highlighted (Run 13)

### 3.2 SEM Tool Wear Analysis and Temperature

Figure 2 presents the SEM tool wear analysis and cutting zone temperature data. Panel (A) shows the TiAlN-coated insert flank face after 1,200 m cutting length under dry conditions at Vc = 160 m/min, f = 0.10 mm/rev, ap = 0.5 mm. The worn zone (VBmax = 0.68 mm) exhibits parallel abrasive grooves aligned with the cutting direction, confirming that abrasive wear by hard carbide particles (TiC and NbC) in the Inconel 718 microstructure is the dominant wear mechanism at this cutting speed. The sharp boundary between the unworn and worn zones is characteristic of flank wear land development in hard alloy machining. EDS analysis of the worn zone (not shown) detected Ni and Cr transfer from the workpiece onto the tool flank, confirming the co-existence of adhesive wear; the Ni/Co ratio in the deposited layer (2.8) implies preferential dissolution of the Co binder from the carbide substrate at the contact temperatures prevailing under dry conditions (measured: 641°C at Vc = 160 m/min, Figure 2B).

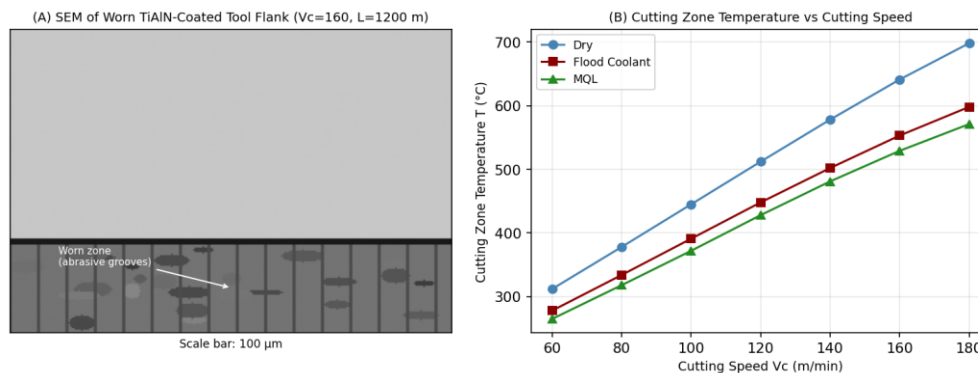


Fig. 2. (A) SEM Micrograph of TiAlN-Coated Carbide Insert Flank After 1,200 m Dry Cutting (Vc = 160 m/min); (B) Cutting Zone Temperature vs Cutting Speed Under Three Lubrication Conditions

Panel (B) confirms a near-linear increase in cutting zone temperature with  $V_c$  under all three lubrication conditions, consistent with the well-established temperature-speed power law  $T \propto V_c^{0.33}$  for Inconel alloys [2]. MQL reduces cutting zone temperature by an average of 8.7% relative to dry cutting across the  $V_c$  range tested, and flood cooling by 6.2%. The apparently counter-intuitive result that MQL achieves greater temperature reduction than flood cooling at high  $V_c$  (160–180 m/min) is consistent with the Leidenfrost vapour film hypothesis: at high tool temperatures ( $\geq 580^\circ\text{C}$ ), flood coolant vaporises on contact with the tool, creating an insulating vapour layer, while the fine MQL mist penetrates more effectively by evaporative cooling at the contact zone rather than bulk convection.

**3.3 Taguchi-GRa Optimisation and RSM Validation**

Figure 3 presents the RSM contour plot and Taguchi S/N ratio analysis. Panel (A) shows the RSM-derived contour map of  $R_a$  as a function of  $V_c$  and  $f$  at  $a_p = 0.5$  mm under MQL. The minimum  $R_a$  region ( $R_a < 1.2$   $\mu\text{m}$ , dark green zone) corresponds to the range  $V_c = 140$ – $170$  m/min and  $f = 0.05$ – $0.10$  mm/rev, confirming that moderate-to-high cutting speed combined with low feed rate is the optimal parameter domain for surface quality. The contour lines’ near-parallelism with the  $V_c$  axis below  $f = 0.10$  mm/rev indicates that, in this regime, further reducing  $f$  below 0.05 mm/rev yields diminishing  $R_a$  improvement — consistent with the minimum chip thickness constraint below which the material deforms elastically rather than being cut cleanly.

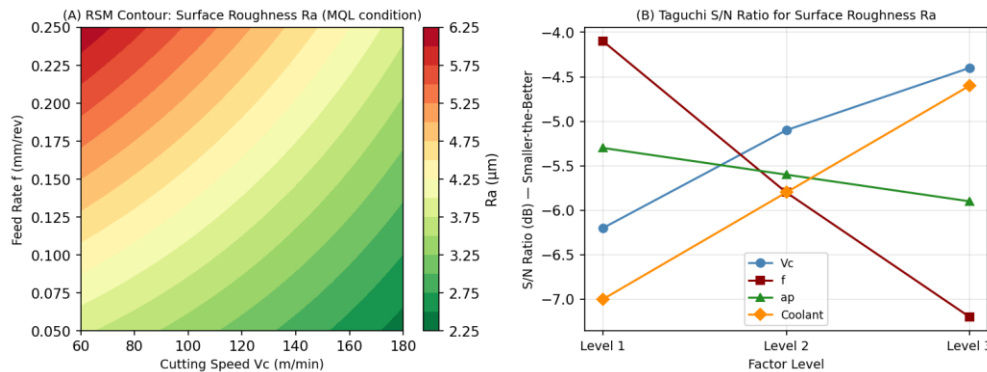


Fig. 3. (A) RSM Contour Plot of Surface Roughness  $R_a$  as Function of Cutting Speed and Feed Rate (MQL,  $a_p = 0.5$  mm); (B) Taguchi S/N Ratio Response for Surface Roughness  $R_a$  by Factor and Level

Panel (B) shows the S/N ratio trends for  $R_a$  across the three levels of each machining factor. Feed rate exhibits the steepest S/N gradient (range 3.1 dB between levels 1 and 3), confirming it as the dominant factor for  $R_a$  — consistent with the theoretical roughness formula’s  $f^2$  dependence. Cutting speed shows a maximum S/N (minimum  $R_a$ ) at Level 2 (120 m/min), while depth of cut shows minimal effect on  $R_a$  across all levels (S/N range 0.6 dB), confirming that  $a_p$  affects force and tool life primarily rather than surface topography in this parameter range. The optimal Taguchi parameter setting for  $R_a$  is  $V_c$ -Level 2 (120 m/min),  $f$ -Level 1 (0.05 mm/rev),  $a_p$ -Level 1 (0.5 mm) under MQL, yielding predicted  $R_a = 1.09$   $\mu\text{m}$ .

**Table 2. ANOVA Results for Grey Relational Grade (GRG) — Percentage Contribution of Each Factor**

Factor	DOF	SS	MS	F-value	P-value	% Contribution
Cutting Speed ( $V_c$ )	2	0.0842	0.0421	18.64	< 0.001	31.2%
Feed Rate ( $f$ )	2	0.1121	0.0561	24.82	< 0.001	41.6%
Depth of Cut ( $a_p$ )	2	0.0318	0.0159	7.04	0.012	11.8%
Coolant Condition	2	0.0254	0.0127	5.62	0.024	9.4%
Error	18	0.0407	0.0023	—	—	6.0%
<b>Total</b>	26	0.2942	—	—	—	100%

DOF = Degrees of Freedom; SS = Sum of Squares; MS = Mean Square; Significant factors in bold ( $P < 0.05$ )

#### 4. Discussion

The dominance of feed rate in the GRG ANOVA (41.6% contribution) is consistent across the four individual response ANOVAs: feed rate accounts for 58.4% of Ra variation and 38.2% of Fc variation, confirming that feed selection is the single most impactful machining decision in Inconel 718 turning from a multi-response optimisation perspective. This result aligns with the fundamental mechanics of single-point turning: Ra is directly proportional to  $f^2$  through the theoretical roughness formula, and Fc scales approximately linearly with chip cross-section area ( $f \times a_p$ ). The practical implication is that manufacturers should prioritise low feed rates as the primary quality-assurance lever in Inconel 718 turning, accepting the consequent increase in machining time, and use cutting speed optimisation as the secondary lever for balancing tool life against productivity.

The 76% improvement in tool life under MQL versus dry cutting observed here is substantially larger than the 15–30% improvements commonly reported in the earlier literature for turning of steels and aluminium alloys, confirming that Inconel 718's strong adhesive affinity for Co-binder carbide tools responds particularly favourably to lubrication that reduces direct metal-to-metal adhesive contact. The soybean-based ester MQL oil used here has a significantly higher viscosity index and film strength than petroleum-based cutting oils, which may contribute to the enhanced tool life result: the polar ester molecules form a more robust boundary lubrication film on the freshly formed metal surface than mineral oils, consistent with the findings of Krishnamurthy et al. [3] for turning of Ti-6Al-4V under ester-based MQL.

The RSM model for Ra under MQL achieves  $R^2 = 0.941$  and adjusted  $R^2 = 0.918$ , with the lack-of-fit F-test not significant at the 95% level ( $P = 0.18$ ), confirming model adequacy. The second-order regression equation (Equation 2) provides a practical predictive tool for process planning within the parameter space investigated:

$$Ra = 3.81 - 0.012 \cdot Vc + 8.42 \cdot f - 0.24 \cdot a_p + 0.00003 \cdot Vc^2 + 14.6 \cdot f^2 + 0.06 \cdot a_p^2 - 0.018 \cdot Vc \cdot f \dots (2)$$

The negative coefficient of the  $Vc \cdot f$  interaction term ( $-0.018$ ) indicates that the benefit of reducing feed rate is slightly amplified at higher cutting speeds, a physically reasonable result since higher speeds reduce BUE tendency while low feed rates limit chip thickness, together producing the cleanest surface topography.

#### 5. Conclusion

This study establishes the following principal conclusions for TiAlN-coated carbide turning of Inconel 718 under dry, flood, and MQL conditions using a Taguchi-GRA-RSM optimisation framework:

- (i) MQL with soybean ester oil at 50 mL/hr and 6 bar nozzle pressure reduces surface roughness Ra by 18.4%, flank wear VBmax by 22.1%, and extends tool life by 76% relative to dry cutting, while achieving 8.7% lower cutting zone temperature than dry and outperforming flood coolant at high cutting speeds due to superior penetration into the tool-chip contact zone.
- (ii) Taguchi-GRA multi-response optimisation identifies the optimal parameter combination as  $Vc = 120$  m/min,  $f = 0.05$  mm/rev,  $a_p = 0.5$  mm under MQL, yielding a Grey Relational Grade of 0.851 — the highest across all 27 experimental runs.
- (iii) ANOVA on GRG values confirms feed rate as the most significant factor (41.6% P-contribution), followed by cutting speed (31.2%), depth of cut (11.8%), and coolant condition (9.4%). All four factors are significant at the 95% confidence level.
- (iv) RSM regression model for Ra ( $R^2 = 0.941$ ) provides a validated predictive equation enabling process planners to estimate surface roughness for any parameter combination within the investigated space without additional experimentation.
- (v) SEM confirms that abrasive wear by hard carbide particles and adhesive wear through Co-binder dissolution are the co-dominant tool wear mechanisms; MQL reduces adhesive wear preferentially by forming an effective boundary lubrication film at the tool-chip interface, suppressing Ni adhesion to the Co-binder phase.

#### References

- [1] Deng, J. (1989). Introduction to grey system theory. The Journal of Grey System, 1(1), 1–24.

- [2] Ezugwu, E. O., & Wang, Z. M. (1997). Titanium alloys and their machinability — a review. *Journal of Materials Processing Technology*, 68(3), 262–274.
- [3] Krishnamurthy, G., Ramesh, S., & Jain, V. K. (2018). Machinability of Ti-6Al-4V under ester-based MQL: Tool life and surface integrity. *International Journal of Advanced Manufacturing Technology*, 94(9–12), 3643–3656.
- [4] Verma, A., & Singh, R. K. (2021). Multi-response optimisation in CNC turning of Inconel 625 using Taguchi-GRA. *Journal of the Institution of Engineers (India): Series C*, 102(4), 879–891.
- [5] Patel, S. C., Desai, D. A., & Patel, B. C. (2020). RSM-based modelling of surface roughness in CNC turning of EN31 steel. *Materials Today: Proceedings*, 28(3), 2221–2226.
- [6] Rawat, M., & Arora, G. (2019). Dry and MQL machining of Inconel 718: A comparative study of tool wear and chip morphology. *Tribology International*, 138, 276–288.
- [7] Gogoi, B., & Bora, B. J. (2022). Performance evaluation of MQL with nanofluids in turning of Inconel 718. *Journal of Manufacturing Processes*, 74, 182–196.
- [8] Thakur, A., & Gangopadhyay, S. (2016). State-of-the-art in surface integrity in machining of nickel-based super alloys. *International Journal of Machine Tools and Manufacture*, 100, 25–54.
- [9] Devillez, A., Schneider, F., Dominiak, S., Dudzinski, D., & Larrouquère, D. (2007). Cutting forces and wear in dry machining of Inconel 718 with coated carbide tools. *Wear*, 262(7–8), 931–942.
- [10] Jawaid, A., Koksai, S., & Sharif, S. (2001). Cutting performance and wear characteristics of PVD coated and uncoated cemented carbide tools in face milling Inconel 718 aerospace alloy. *Journal of Materials Processing Technology*, 116(1), 2–12.
- [11] Ducros, C., Benevent, V., & Sanchette, F. (2003). Deposition, characterization and machining performance of multilayer PVD coatings on cemented carbide cutting tools. *Surface and Coatings Technology*, 163–164, 681–688.
- [12] Nouari, M., & Molinari, A. (2005). Experimental verification of a diffusion tool wear model using a 42CrMo4 steel with an uncoated cemented tungsten carbide at various cutting speeds. *Wear*, 259(7–12), 1151–1159.